processes

MDPI

Article

The Impact of Weld Repairs on the Microstructure and Mechanical Integrity of X80 Pipelines in Oil and Gas Transmission

Lifeng Li [1,2,*], Lixia Zhu [2], Xiangzhen Yan [1], Haidong Jia [3], Shuyi Xie [2] and Yangfan Zou [2]

[1] College of Pipeline and Civil Engineering, China University of Petroleum (East China), Qingdao 266580, China
[2] State Key Laboratory of Oil and Gas Equipment, Tubular Goods Research Institute of CNPC, Xi'an 710077, China
[3] West Pipeline Company of Pipe China, Urumqi 830013, China
* Correspondence: lilifeng004@cnpc.com.cn

Abstract: The integrity of oil and gas pipelines is critical to energy transportation and has significant implications for national energy security. This study employs finite-element numerical simulation to investigate the impact of multiple repairs on the microstructure and mechanical integrity of X80 pipeline girth welds. The effects of varying repair iterations on the microstructure, toughness, and loading capacity of high-strength steel pipes were analyzed. The results revealed that the microstructure of the welded joint remained unchanged across different repair instances, but the toughness, optimized by welding heat input, diminished after three repairs due to grain growth from repeated thermal cycles. Specifically, the impact toughness of the welding line, fusion line, and adjacent areas decreased significantly after three repairs, with the toughness of the welding line dropping to 25 J and the fusion line dropping to 30 J. The hardness of the welded joint decreased with repairs, and the dispersion of hardness increased. The average hardness at the welding line decreased from 25 HV to 20 HV after three repairs. Residual stress in the repaired girth weld was highest in the filling welding layer, increasing with the number of repairs. The loading capacity of the girth weld significantly decreased after the first repair (by 12.1%) and continued to decrease with additional repairs (15.3% after the second repair and 16.7% after the third repair). It is concluded that X80 pipeline girth welds should be repaired no more than twice to maintain optimal structural integrity.

Keywords: repair instance; microstructure; loading capacity; numerical simulation; energy security

check for updates

Academic Editor: Qingmin Yu

Received: 26 December 2024
Revised: 8 February 2025
Accepted: 11 February 2025
Published: 12 February 2025

Citation: Li, L.; Zhu, L.; Yan, X.; Jia, H.; Xie, S.; Zou, Y. The Impact of Weld Repairs on the Microstructure and Mechanical Integrity of X80 Pipelines in Oil and Gas Transmission. *Processes* **2025**, *13*, 512. https://doi.org/10.3390/pr13020512

Copyright: © 2025 by the authors. Licensee MDPI, Basel, Switzerland. This article is an open access article distributed under the terms and conditions of the Creative Commons Attribution (CC BY) license (https://creativecommons.org/licenses/by/4.0/).

1. Introduction

Oil and gas pipelines are integral to the global energy infrastructure, facilitating the transportation of hydrocarbon resources over long distances and playing a pivotal role in energy supply chains. The integrity of these pipelines, particularly the girth welds in high-strength steel such as X80, is crucial for the safe and efficient conveyance of oil and gas. Weld quality is very important, as it has significant implications for energy security and the reliability of national energy distribution networks [1]. The incidence of pipeline failures, often attributed to weld defects, highlights the need for advanced welding techniques and effective repair strategies.

Nowadays, the development of the welding technique has significantly improved the construction, quality, and efficiency in oil and gas pipeline sites. However, girth weld

repair caused by unqualified welds is still unavoidable. In recent years, failure accidents of oil and gas pipelines caused by girth welds have occurred frequently [1,2]. More than 70% of the over 30 pipeline failures that occurred at the onset of high-grade steel operations, including the second line of the West-to-East Gas Pipeline, the Mohe–Daqing Gas Pipeline, and the third Gas Pipeline of Shaanxi–Beijing, were attributed to girth weld defects [3]. These incidents underscore the critical role of welding quality in ensuring the integrity and safety of oil and gas pipelines, which are vital arteries for energy transportation and thus crucial to national energy security.

Previous studies have investigated the effects of multiple repairs on the mechanical properties and microstructure of welded joints. For example, Vega et al. [4] studied the impact of multiple shielded metal arc welding repairs on the mechanical properties of girth welds in seamless API X52 steel pipes. They found that, despite grain growth in the heat-affected zone, the weld joints maintained compliance with the API 1104 standard [5] after up to four repairs. Bouchard et al. [6] analyzed the residual stress in a stainless steel pipe girth weld containing long and short repairs using various measurement techniques, including neutron diffraction, deep hole, and surface hole methods. They found that residual stresses located at the mid-length of the heat-affected zone were higher in the short repairs compared to the long repairs and that repair welds significantly altered the through-wall stress profiles compared to the original girth weld. Kollar et al. [7] summarized the effects of repair welding during manufacturing on residual stresses, distortions, and plastic strains in T-joints using numerical modeling, highlighting the significant impact of rewelding sequence, heat input, and weld size on these parameters. They found that repair welding can lead to an approximate 33% increase in plastic strain and a 26% increase in von Mises residual stress peak at the weld extremity, emphasizing the importance of avoiding repair welding to maintain structural integrity. Chen et al. [8] studied the through-thickness residual stress distribution in AISI 316L pipelines with and without repair welding, developing a welding pass size merging strategy to efficiently analyze the effects of the component radius-to-wall thickness ratio and the heat input on the welding stress profiles. They established analytical equations for predicting residual stress in both original and repaired welds, demonstrating that a smaller repair depth led to more efficient improvements in residual stress distribution.

Domestic and foreign oil and gas pipeline standards assert the following claim: API 1104 “Welding of Pipelines and the Welding of Related Accessories” requires qualified welding technology to be applied to the welding repair, and the second repair should be agreed with the owner. Appendix C of the DNV-OS-F101 “Code for Submarine Pipelines” [9] states that the welding line can be repaired twice. GB/T 50369 “Code for Construction and Acceptance of Oil and Gas long-distance Pipeline Engineering” [10] outlines the fact that the welding line can be repaired no more than twice in the same zone, and the root welding line should be allowed to be repaired once. These standards reflect the importance of maintaining the structural integrity of pipelines to safeguard the uninterrupted flow of energy resources.

Researchers from various countries have also studied the time taken to repair the welding line. Vega et al. [4] found that multiple repairs significantly influence the mechanical properties of girth welds in X52 seamless steel pipes. Specifically, they observed that, after four repairs, the impact toughness of the weld joint decreased by 20% compared to the initial state, while the hardness in the heat-affected zone (HAZ) increased by 15 HV. These changes were attributed to grain growth and the formation of Widmanstätten ferrite in the HAZ. Moeinifar et al. [11] investigated the effects of thermal cycles, including both actual and simulated (Greeble) conditions, on the microstructure and mechanical properties of welded joints. Their study revealed that the presence of martensite/austenite (M/A)

constituents significantly affected the mechanical properties of the reheating position in thermal simulations. They found that a higher volume fraction of M/A constituents led to a 30% increase in hardness but a 25% decrease in toughness, highlighting the critical role of these constituents in determining the mechanical behavior of the welds. Vitasek [12] studied the impact of multiple repairs on the quality of oil and gas pipeline weld joints and found that the weld joint quality deteriorated with increasing repair instances. Specifically, after three repairs, the average grain size in the HAZ increased from 20 μm to 30 μm, and the impact toughness dropped from 40 J to 25 J. These findings underscore the importance of limiting the number of repairs to maintain structural integrity. In addition, most studies have focused on the effects and distribution of residual stress in welding repairs using finite-element modeling [6,7,13–15], which is crucial for understanding the long-term integrity of pipelines and their contribution to energy security.

In this study, the finite-element numerical simulation method is used to analyze the effects of several repairs on the microstructure, toughness, and loading capacity of high-grade steel pipes, providing guidance for pipeline construction and complete theoretical support for the repair of pipe welds. This research is particularly relevant in the context of energy security, as it aims to enhance the safety and reliability of oil and gas pipelines, thereby ensuring the stable supply of energy resources.

2. Experimental Materials and Methods

2.1. Experimental Procedures

Table 1 shows the nominal chemical composition of X80. For the X80 pipe ring weld with a diameter of 1219 mm and a wall thickness of 18.4 mm, a V groove was machined in the center of the weld and then repaired according to the standard GB/T 50369. During the repair process, a K-type thermocouple was used to measure the thermal cycle curve. A Gleeble 3500 thermodynamic simulation test system, manufactured by Dynamic Systems Inc., Albany, NY, USA, was used to apply heat inputs 1, 2, and 3 times to the welds based on heat cycles measured from actual repaired welds. The heating rate was 146 °C/s, the peak temperature was 1150 °C, which was held for 1 s, and the $T_{8/5}$ time was 10 s. The interlaminar temperature was controlled at 100 °C. The microstructure of different locations of the welding line was observed, and a −15 °C Charpy impact test (V-notch) was performed according to samples derived at different times of the heating input. Vickers hardness measurements were performed on the cross-section using a KB30BVZ-FA automatic hardness tester (Shanghai Kehua Testing Equipment Co., Ltd., Shanghai, China) under a load of 500 g for 10 s. The morphology of the weld joint after repair simulation is shown in Figure 1. The welding line and heat-affected zone (HAZ) widths were 6~7 mm and 2.5~4 mm, respectively. The gaps of the impact specimen were distributed in the center of the welding line, fusion line, fusion line + 1 mm, fusion line + 2 mm, and fusion line + 3 mm. Among them, the fusion line was in the boundary between the HAZ of the coarse grain and fine grain, while the fusion line + 2 mm was in the HAZ of the fine grain, and the fusion line + 3 mm was in the base material.

Table 1. Nominal chemical composition of X80 steel (wt.%).

C	Si	Mn	P	S	Cr	Mo	Ni	Nb	V	Ti	Cu	Al
0.05	0.21	1.84	0.013	0.002	0.28	0.28	0.056	0.078	0.026	0.016	0.062	0.033

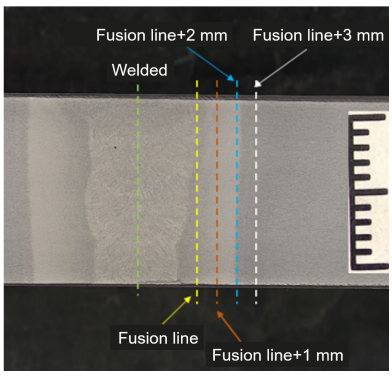


Figure 1. The weld joint after the repair.

2.2. Establishment of the Model

Abaqus was used to simulate the temperature distribution and residual stress of the girth weld under different repairs. Primarily, the girth weld model was built based on the morphology of the weld joint; then, material properties were assigned to each area and we made use of the heat source model and Fortran language to load the welding heat source to obtain the temperature field and thermal cycle in the heat source process. The calculation of the residual stress was mainly completed by importing the temperature field. To ensure that the grid of the temperature and residual stress kept the same unit and node and avoid the calculus of the interpolation caused by inconsistent units, it was reasonable for the properties of the grids to be changed to a three-dimensional stress unit. Thus, we repaired the girth weld model and reheated it 1, 2, and 3 times to obtain measures of the stress field under different repair iterations.

The method of "sequential coupling" was used to simulate the temperature distribution, residual stress, and strain of the welded joints using ABAQUS. In "sequential coupling", the sequence "temperature–stress–strain" was followed in the numerical calculation. The temperature distribution of the pipe was derived from the thermal calculation results and used as a predefined field for calculating the distribution of the stress field, thus executing the accurate prediction of the residual stress field of the welded joint. In addition, "model change" was used to simulate the actual filling process of the welded joint. The material was X80 pipeline steel with a diameter and wall thickness of 1219 mm and 18.4 mm, respectively. To improve the computational efficiency, only 1/8 of the pipe was modeled. The mesh near the center of the weld and the heat-affected zone was refined, while the mesh away from the weld was divided more sparsely, as shown in Figure 2. All weld meshes were deleted before welding, and each layer of the mesh was gradually activated during welding until the latter was completed. To increase the accuracy of the calculations, a reliable heat transfer model needed to be constructed. The double-ellipse heat source model possesses high accuracy and stability when performing manual arc welding and submerged arc welding, so it was selected as the heat source.

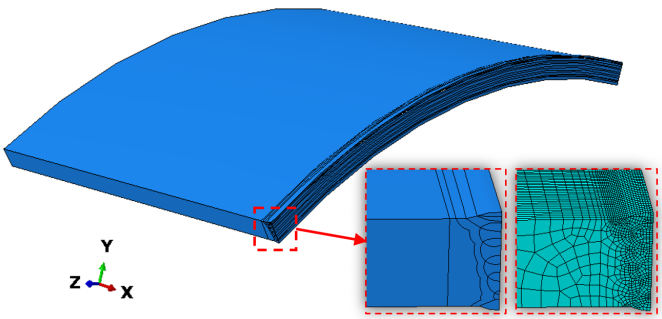


Figure 2. Modeling and meshing.

To analyze the temperature distribution of the joint, the temperatures on different paths were extracted from the model. The paths were set as shown in Figure 3a,b, along the thickness and width directions, respectively. Welding is a complex coupling process of heat and force, so the effect of the material's thermophysical properties with ambient temperature variations must be considered. The thermophysical parameters and mechanical properties of X80 used in this study referred to the existing literature [16]. In addition, symmetry boundary conditions were applied on the planes of symmetry to constrain displacements perpendicular to these planes, ensuring model symmetry. Heat flux was applied at the weld location to simulate the welding process, with heat transfer allowed across symmetry planes. These conditions ensured that the model accurately reflected the real-world scenario while maintaining computational efficiency.

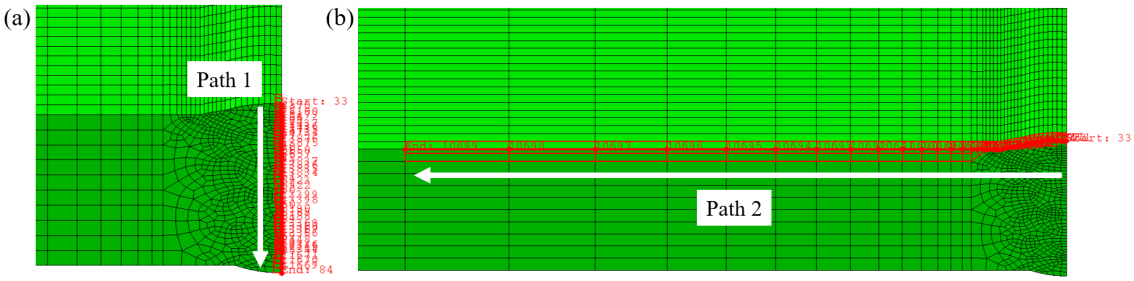


Figure 3. Schematic diagram of the temperature measurement path: (**a**) path 1, (**b**) path 2.

3. Results and Discussion

3.1. Microstructure

The microstructures of the weld zone (WZ) and HAZ after zero, one, two, and three repairs are shown in Figures 4 and 5, and the microstructure types did not change under different repairs. The microstructure of the WZ was mainly intracrystalline nucleation acicular ferrite and massive pre-eutectic ferrite. Before repair, there were obvious columnar crystals in the WZ, massive pre-eutectic ferrite precipitated along the grain boundaries of the columnar crystals, and a small amount of Widmanstatten microstructures spanning from the grain boundaries to the intracrystalline growth. With the increase in the number of repairs, the first eutectic ferrite content in WZ increased slightly. After three repairs, the first eutectic ferrite in WZ increased significantly; the grain size also increased, accompanied by more Widmanstatten microstructures. The microstructure of the HAZ in the coarse grains mainly comprised granular bainite. With the increase in repair instances, the component distribution of the M/A changed, and its distribution gradually became uniform along the slats in the crystal. As a result, the properties of direction were weakened. In addition, with the increase in repairs, the average size of the coarse grains in the HAZ also changed. The initial average grain size was about 32 μm, and it was uniform. The average grain size was about 25 μm after one repair, but the dispersity of the grain increased. After two repairs, the sizes were reduced to 12 μm, and the grains were generally uniform. After three repairs, the average size became 15 μm, and there were some large grains locally. The results show that multiple repairs on the WZ and HAZ had a superposition effect. The effect of welding heat input caused grain recrystallization and refinement [17], and with the repeated heating and cooling effects produced by thermal cycling, the progressively refined grains started growing again, with the microstructure of the WZ and HAZ degradation occurring in the third thermal cycle.

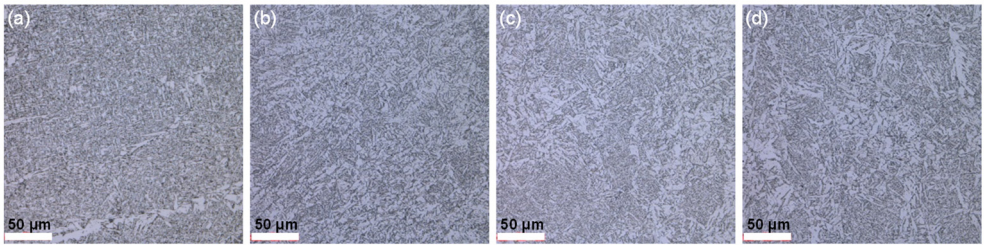


Figure 4. Microstructure of the WZ after different repair instances: (**a**) zero, (**b**) one, (**c**) two, and (**d**) three repairs.

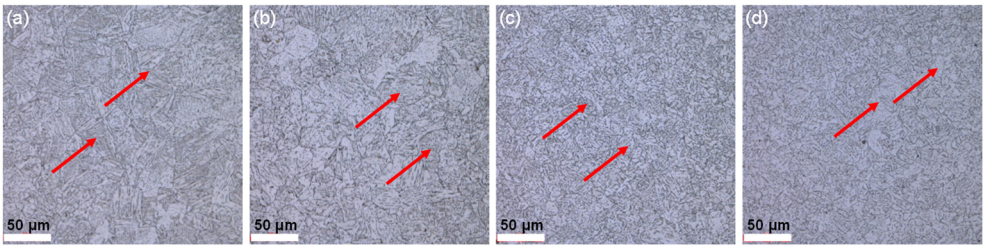


Figure 5. Microstructure of HAZ after different repair instances: (**a**) zero, (**b**) one, (**c**) two, and (**d**) three repairs.

3.2. Toughness

The impact toughness of X80 steel pipe ring welds after different instances of repair is shown in Figure 6. The results show that, regardless of the number of repair instances, toughness near the weld was the worst, followed by that of the fusion line. Figure 6 shows the change in the impact toughness of the X80 pipeline girth weld after zero, one, two, and three repairs, respectively. It can be found that the toughness near the welding line was the worst, followed by that near the fusion line. The toughness of the fusion line was consistent under different repair instances, which could be explained by the fact that the granular bainite microstructure located on the fusion line was relatively thick and that the M/A component size within the crystal was significant, its arrangement having specific directions not conducive to toughness. After the repair, the impact toughness at the fusion line did not fluctuate. Instead, it increased slightly owing to the refined microstructure of granular bainite formed after the second repair and the uniform grains. The first and second repairs improved the impact toughness of the welding line, fusion line + 1 mm, fusion line + 2 mm, and fusion line + 3 mm. However, after three repair instances, the microstructure of different locations worsened due to the cumulative effect brought about by the repeating welding thermal cycle, making the impact toughness of the welding line, fusion line + 1 mm, fusion line + 2 mm, and fusion line + 3 mm decrease to a lower degree than the initial value.

The observed sudden change in impact energy for the first and second repair conditions in the fusion line and HAZ regions could be attributed to the microstructural transformations induced by repeated thermal cycles during the repair process. Specifically, after the first repair, the microstructure in these regions underwent significant changes, including grain refinement and the formation of finer bainitic structures. These microstructural changes generally improved the toughness, as evidenced by the increased impact energy. However, after the second repair, further grain growth and the development of more complex microstructures, such as Widmanstätten ferrite, occurred. These changes led to a decrease in toughness, resulting in a drop in the impact energy [18].

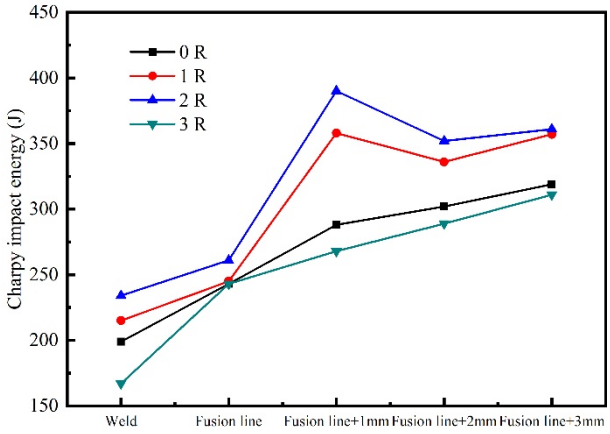


Figure 6. Impact toughness of weld joint after different repair instances.

3.3. Hardness

In Figure 7, the effects of different repair instances on the hardness of the welding line, HAZ, and base material are illustrated. The first repair decreased the hardness significantly, while several repairs could improve the hardness slightly based on the first repair, but the degree of improvement was not apparent. Ignoring the repair instances, the hardness at the welding line and HAZ was lower than that calculated in the base material, indicating that all weld joints had softened noticeably, and the lowest hardness appeared at the welding line.

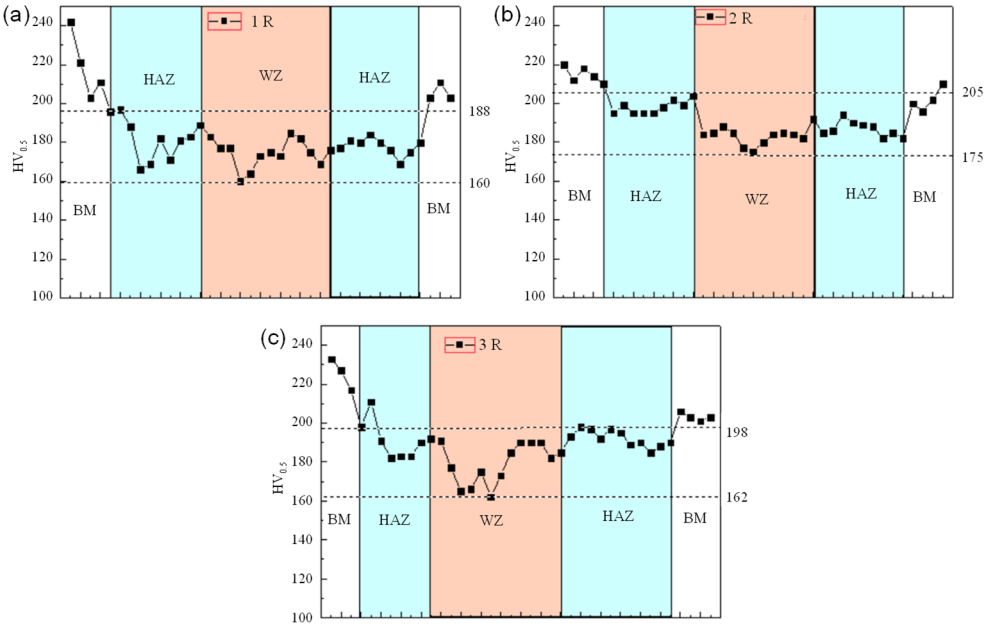


Figure 7. Hardness of weld joint after different repair instances: (**a**) one, (**b**) two, and (**c**) three repairs.

The dispersibility of the hardness at the welded HAZ and that calculated in the base material were analyzed statistically, and the results are shown in Table 2. The number of repairs had little impact on the distribution of the hardness along the welding line, but the repairs increased the dispersibility of the hardness at the HAZ and in the base material. During the process of repair, the microstructures in the HAZ and base material were influenced by the heat input, the phase content, and the grain size change, making the dispersibility at the HAZ and base material increase.

The lower hardness observed in the welding line and HAZ compared to the base material was due to the significant heat input and rapid thermal cycling during the welding process. These conditions led to microstructural changes, such as grain growth and the for-

mation of softer phases, which resulted in a softer material. The welding line, experiencing the most intense heating and cooling, showed the lowest hardness values.

Table 2. The dispersibility of the hardness after different repair instances in different zones.

Area	Welded	Repaired Once	Repaired Twice	Repaired Three Times
WZ	25	25	29	27
HAZ	27	44	43	29
BM	8	39	24	40

3.4. Temperature Distribution

To ensure the accuracy of our simulation results, we conducted experimental validation of the temperature curves. The thermal cycle curves measured during the welding repair process using a K-type thermocouple were used as input for our finite-element numerical simulations. This validation step confirmed that our simulation model accurately captured the thermal conditions experienced during the actual welding repairs, as shown in Figure 8.

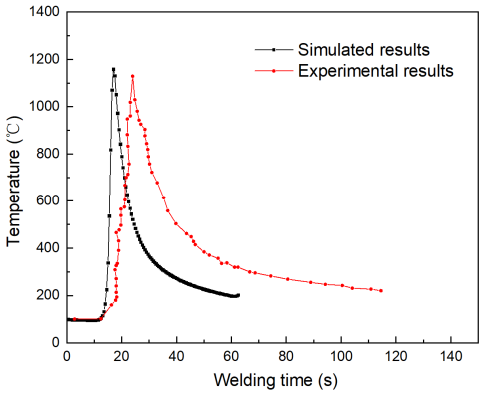


Figure 8. Heating input curve of the welding repair.

Figure 9 shows the temperature distribution of the welded joint at different stages. As the heat source moves forward, the metal in front of the heat source is continuously heated, leading the material temperature to gradually increase and form a stable molten pool. The temperature of the metal behind the heat source gradually decreases due to heat transfer to the base metal, and the difference in temperature distribution between the weld zone and the base metal of the weld gradually increases. Eventually, the heat in the weld zone is transferred to the base metal by heat conduction and to the air by convective heat transfer. The temperature is highest in the center of the area where the heat source acts and gradually decreases farther away from the center of the heat source. In addition, the material is gradually activated as the heat source is moved, which is more in accordance with the actual welding process.

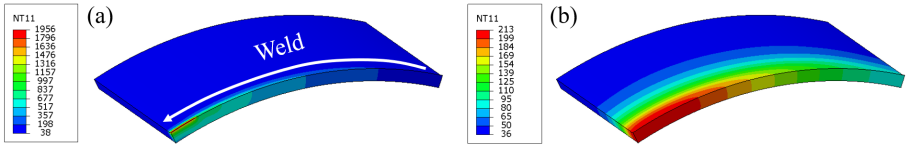


Figure 9. Temperature distribution (**a**) after welding and (**b**) after cooling.

Figure 10 shows the temperature distribution of the joints corresponding to different numbers of repairs. Since the specimens were cooled to room temperature before each repair, there was no significant difference in the temperature distribution of the joints undergoing different numbers of repairs.

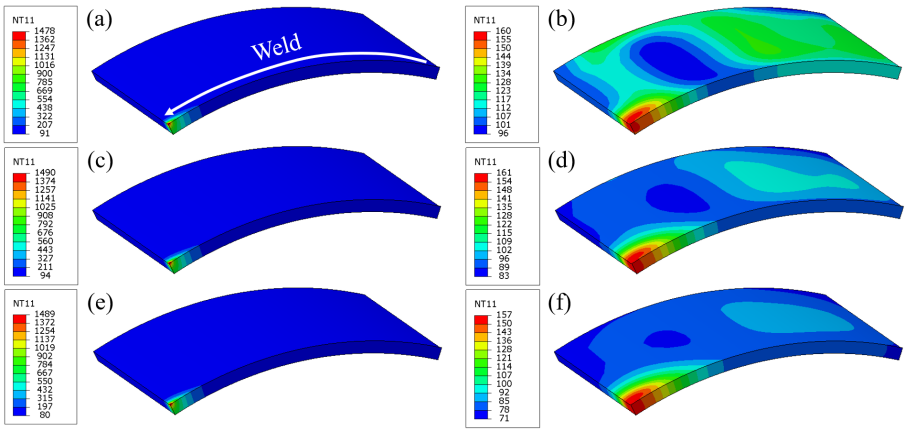


Figure 10. Temperature distribution at different repair times: (**a**) repaired once, after welding; (**b**) repaired once, after cooling; (**c**) repaired twice, after welding; (**d**) repaired twice, after cooling; (**e**) repaired three times, after welding; and (**f**) repaired three times, after cooling.

Figure 11a–d show the temperature distribution in the thickness direction of the joint for the following conditions: welding, repairing once, repairing twice, and repairing three times, respectively. The temperature in the thickness direction at the center of the welded joint decreased as the distance increased from the upper surface after welding. The temperature at the upper surface was the highest, about 1800 °C. The temperature at the lower surface was about 510 °C. The temperature gradient in the thickness direction of the joint was large. After cooling, the temperature of the joint decreased significantly, and the temperature difference between the upper and lower surfaces decreased. As for the temperature distribution under different repair instances, there was no significant difference. After the repair, the peak temperature in the thickness direction was still found on the upper surface of the welded joint, about 1480 °C. The temperature distribution in the thickness direction was almost uniform after cooling.

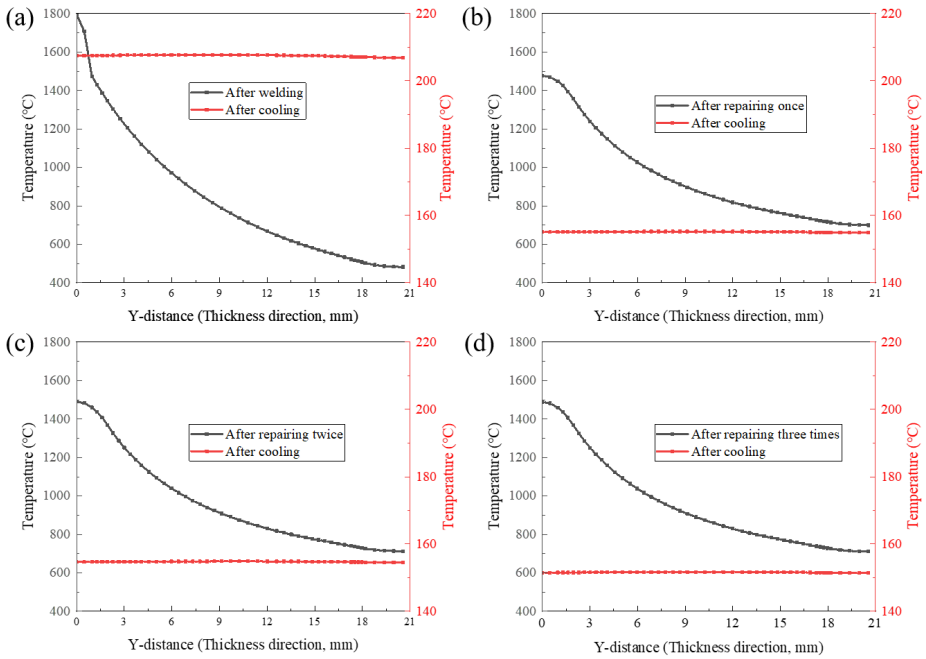


Figure 11. Temperature distribution in thickness direction (Y-distance): (**a**) welding, (**b**) repaired once, (**c**) repaired twice, and (**d**) repaired three times.

Figure 12 shows the temperature distribution at different distances from the center of the joint. The temperature was highest at the center and decreased rapidly from the

center of the joint outward. After cooling, the peak temperature and the temperature gradient decreased, but the temperature tended to be uniform. Since the joint experienced sufficient cooling before each repair, there was no significant difference in the temperature distribution found in the joint after different repair instances.

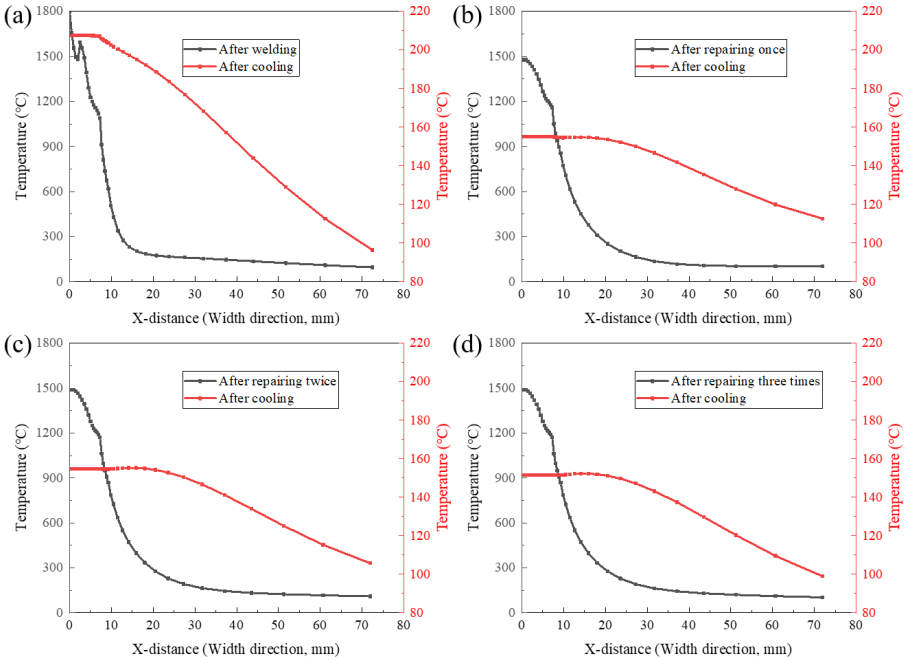


Figure 12. Temperature distribution in the width direction (X-distance): (**a**) welding, (**b**) repaired once, (**c**) repaired twice, and (**d**) repaired three times.

3.5. The Distribution of the Stress Field and Loading Capacity

The loading capacity of the girth weld after different repair instances was simulated, and the residual stress is shown in Figure 13. With the increase in repair instances, the maximum stress value increased slightly. The maximum residual stress varied with the pressure in different zones of the girth weld, as shown in Figures 14 and 15. Residual stress gradually increased from the outer surface cover to the inner surface root weld without repair. The residual stress at the root welding layer was higher than at the other layer. The highest value was located at the extremity of the root welding layer. After one, two, or three repairs, the residual stress at the filling welding layer was higher than at the root welding layer. Based on the strength failure criterion, in the general stress state, when the maximum stress value of the girth weld in the wall thickness of the section reaches the yield strength value, a failure happens, so the loading capacity of the unrepaired girth weld depends on the root welding layer in the general stress state, while the loading capacity of the repaired girth weld depends on the filling welding layer. As the pressure increases, the loading capacity of the girth weld joint also increases. When the maximum value of the residual stress reaches the yield strength, as the stress increases again, the weld joint is deformed, and when the maximum residual stress reaches the tensile strength, the weld joint breaks and fails, and this value is defined as the ultimate pressure. The change in the loading capacity of the girth weld after different repair instances is shown in Figure 15. Compared to the unrepaired girth weld, the first repair reduced the loading capacity by 12.1%. The second repair reduced it by 15.3%, and the third reduced it by 16.7%. The loading capacity decreased significantly after the first repair and decreased slightly with the number of repair instances.

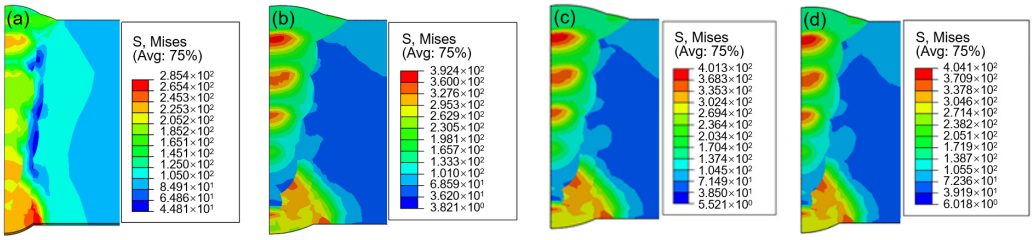


Figure 13. Residual stress of the girth weld after different repair instances: (**a**) zero, (**b**) one, (**c**) two, and (**d**) three repairs.

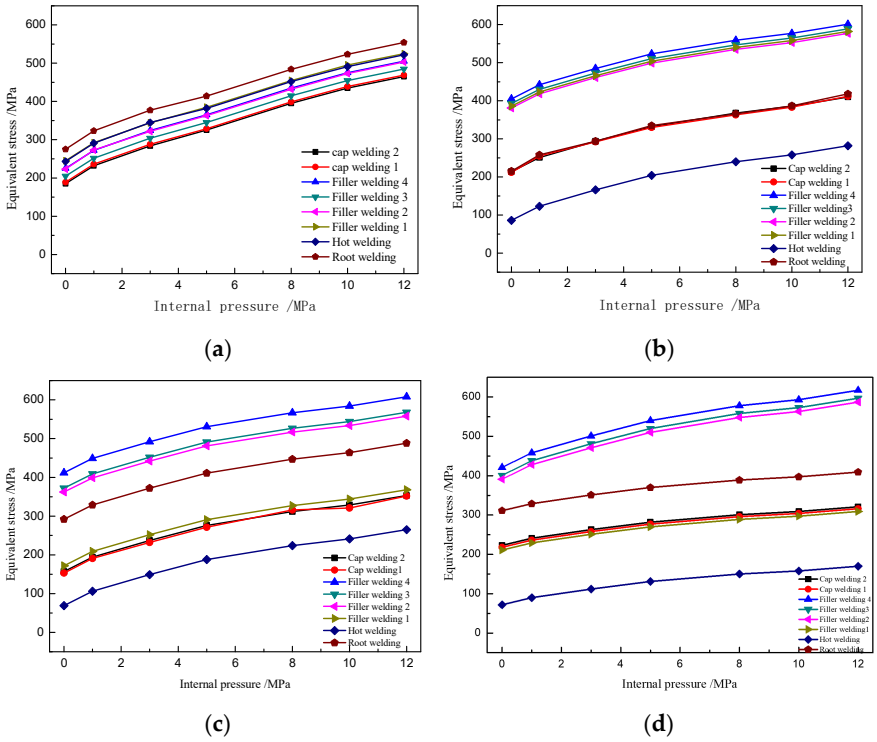


Figure 14. Residual stress at different locations after different repair instances: (**a**) zero, (**b**) one, (**c**) two, and (**d**) three repairs.

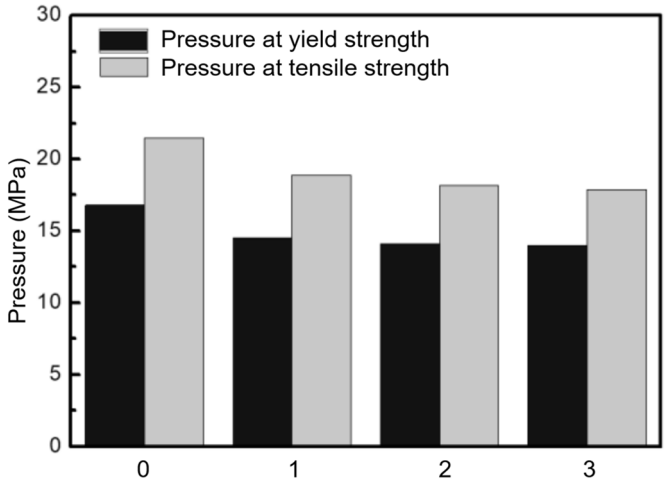


Figure 15. Loading capacity of the girth weld joint after different repair instances.

4. Conclusions

(1) The microstructure of the weld joint remained unchanged across different repair iterations. However, the toughness, optimized by the welding heat input, diminished

after three repairs due to grain growth from repeated thermal cycles. Specifically, the impact toughness of the welding line, fusion line, and adjacent areas decreased significantly after three repairs, highlighting the importance of limiting the number of repairs.

(2) The hardness of the weld joint decreased with repairs, and the dispersion of the hardness values increased. While multiple repairs could marginally enhance the hardness relative to the initial repair, the overall trend was a reduction in hardness, with the lowest values observed at the welding line.

(3) The temperature distribution in the thickness direction of the welded joint showed a significant gradient, with the highest temperature found on the upper surface (about 1800 °C) and the lowest on the lower surface (about 510 °C).

(4) The maximum residual stress after repair was found in the filling welding layer and increased with the number of repairs. The loading capacity of the girth weld decreased significantly after the first repair (by 12.1%) and continued to decrease with additional repairs (15.3% after the second repair and 16.7% after the third repair). This indicated that the first repair had the most significant impact on the loading capacity, and subsequent repairs further reduced it.

Author Contributions: Methodology, H.J.; Investigation, X.Y.; Resources, S.X.; Writing—original draft, L.L.; Writing—review & editing, L.Z.; Visualization, Y.Z. All authors have read and agreed to the published version of the manuscript.

Funding: This research received no external funding.

Data Availability Statement: The original contributions presented in this study are included in the article. Further inquiries can be directed to the corresponding author.

Conflicts of Interest: Authors Lifeng Li, Lixia Zhu, Shuyi Xie, and Yangfan Zou are employed by the Tubular Goods Research Institute of CNPC; Author Haidong Jia is employed by the West Pipeline Company of Pipe China. The remaining author declares that the research was conducted in the absence of any commercial or financial relationships that could be construed as potential conflicts of interest.

References

1. Savari, A. Crack assessment in spiral-welded pipelines repaired by composite patch: A SMART and failure assessment diagram approach. *J. Pipeline Sci. Eng.* **2024**, *5*, 100222. [CrossRef]
2. Alves, D.T.S.; Alves Lima, G.B. Establishing an onshore pipeline incident database to support operational risk management in Brazil-Part 2: Bowtie proposition and statistics of failure. *Process Saf. Environ. Prot.* **2021**, *155*, 80–97. [CrossRef]
3. Wang, B.; Liu, Q.; Feng, Q.S.; Wang, X.; Yang, Z.; Dai, L.; Huo, X.; Wang, D.; Yu, J.; Chen, J. Influence of welding defects on hydrogen embrittlement sensitivity of girth welds in X80 pipelines. *Int. J. Electrochem. Sci.* **2024**, *19*, 100661. [CrossRef]
4. Vega, O.E.; Hallen, J.M.; Villagomez, A.; Contreras, A. Effect of multiple repairs in girth welds of pipelines on the mechanical properties. *Mater. Charact.* **2008**, *59*, 1498–1507. [CrossRef]
5. *API Standard 1104*; Welding of Pipelines and Related Facilities. American Petroleum Institute: Washington, DC, USA, 2005.
6. Bouchard, P.J.; George, D.; Santisteban, J.R.; Bruno, G.; Dutta, M.; Edwards, L.; Kingston, E.; Smith, D. Measurement of the residual stresses in a stainless-steel pipe girth weld containing long and short repairs. *Int. J. Press. Vessel. Pip.* **2005**, *82*, 299–310. [CrossRef]
7. Kollár, D. Numerical modelling on the influence of repair welding during manufacturing on residual stresses and distortions of T-joints. *Results Eng.* **2023**, *20*, 101535. [CrossRef]
8. Chen, Z.H.; Wang, P.; Wang, H.H.; Xiong, Z. Thermo-mechanical analysis of the repair welding residual stress of AISI 316L pipeline for ECA. *Int. J. Press. Vessel. Pip.* **2021**, *194 Pt B*, 104469. [CrossRef]
9. *DNV-ST-F101*; Submarine Pipeline Systems. DNV AS: Porsgrunn, Norway, 2021.
10. *GB/T 50369*; Code for Construction and Acceptance of Oil and Gas Long-Distance Pipeline Engineering. China National Standardization Administration: Beijing, China, 2014.

11. Moeinifar, S.; Kokabi, A.H.; Hosseini, H.R.M. Effect of tandem submerged arc welding process and parameters of Gleeble simulator thermal cycles on properties of the intercritically reheated heat affected zone. *Mater. Des.* **2011**, *32*, 869–876. [CrossRef]
12. Vitasek, M. Multiple repairs of circumferential welded joints in gas pipelines. *Weld. Int.* **1989**, *3*, 168–172. [CrossRef]
13. Vega-Becerra, O.; Galván-Martínez, R.; Hernández-Mejía, S.L.; Contreras-Cuevas, A. Residual stress assessment of multiple welding repairs of girth welds in pipeline used in oil industry. *Mater. Sci. Forum* **2014**, *793*, 93–104. [CrossRef]
14. Dai, P.Y.; Wang, Y.F.; Li, S.; Lu, S.; Feng, G.; Deng, D. FEM analysis of residual stress induced by repair welding in SUS304 stainless steel pipe butt-welded joint. *J. Manuf. Processes* **2020**, *58*, 975–983. [CrossRef]
15. Keivani, R.; Jahazi, M.; Pham, T.; Khodabandeh, A.R.; Afshar, M.R. Predicting residual stresses and distortion during multisequence welding of large size structures using FEM. *Int. J. Adv. Manuf. Technol.* **2014**, *73*, 409–419. [CrossRef]
16. Huang, X.G.; Liu, H.H.; Huang, C.; Cui, J.; Xiao, Z.; Zhu, X. Creep relaxation to relieve residual stress in girth-butt welded X80 pipelines: Simulation and experiment. *Thin-Walled Struct.* **2024**, *205 Pt C*, 112597. [CrossRef]
17. Fu, C.Z.; Tao, C.C.; Huang, H.J.; Zhou, G.; Lin, X.; Zhang, H.; Chen, L.; Yuan, X. Exploring microstructure evolution and machine-learning methods based on SCAT-CIWOA-BP-DMM theory during hot deformation of 56Ni–32Ti–12Hf alloy. *Intermetallics* **2024**, *171*, 108342. [CrossRef]
18. Zuo, Z.Y.; Ma, H.W.; Yarigarravesh, M.; Assari, A.H.; Tayyebi, M.; Tayebi, M.; Hamawandi, B. Microstructure; fractography, and mechanical properties of Hardox 500 Steel TIG-welded joints by using different filler weld wires. *Materials* **2022**, *15*, 8196. [CrossRef] [PubMed]

Disclaimer/Publisher's Note: The statements, opinions and data contained in all publications are solely those of the individual author(s) and contributor(s) and not of MDPI and/or the editor(s). MDPI and/or the editor(s) disclaim responsibility for any injury to people or property resulting from any ideas, methods, instructions or products referred to in the content.